Developmental Cell, Vol. 5, 611–620, October, 2003, Copyright ©2003 by Cell Press

The Claudin-like Megatrachea Is Essential in Septate Junctions for the Epithelial Barrier Function in *Drosophila*

Matthias Behr,[1] Dietmar Riedel,[2] and Reinhard Schuh[1,*]
[1]Abteilung Molekulare Entwicklungsbiologie
[2]Abteilung Elektronenmikroskopie
Max-Planck-Institut für Biophysikalische Chemie
Am Fassberg
37077 Göttingen
Germany

Summary

Vertebrate claudin proteins are integral components of tight junctions, which function as paracellular diffusion barriers in epithelia. We identified Megatrachea (Mega), a *Drosophila* transmembrane protein homologous to claudins, and show that it acts in septate junctions, the corresponding structure of invertebrates. Our analysis revealed that Mega has transepithelial barrier function similar to the claudins. Also, Mega is necessary for normal tracheal cell morphogenesis but not for apicobasal polarity or epithelial integrity. In addition, we present evidence that Mega is essential for localization of the septate junction protein complex Coracle/Neurexin. The results indicate that claudin-like proteins are functionally conserved between vertebrates and *Drosophila*.

Introduction

Most metazoa are subdivided into distinct fluid compartments to establish and maintain homeostasis. The different compartments are separated by epithelial cellular sheets, which dynamically retain the internal environment of distinct body sections. To exert this physiological role, cell sheets must function as barriers to control the paracellular transport of solutes across the layers (Rodriguez-Boulan and Nelson, 1989). In vertebrates, these intercellular barriers are formed in the most apical region of lateral cell membranes in specialized complexes, the tight junctions (TJs). However, TJs do not function merely as simple barriers, but rather mediate regulated diversified permeability depending on physiological requirements and/or cell type (Tsukita et al., 2001; Schneeberger and Lynch, 1992).

Integral components of TJs are claudins, four-transmembrane domain proteins (Furuse et al., 1998a; Morita et al., 1999). The mammalian claudin family contains more than 20 members (Kollmar et al., 2001; Tsukita and Furuse, 2002), which are involved in paracellular permeability (Gow et al., 1999; Simon et al., 1999; Sonoda et al., 1999). Heterogeneous claudin species copolymerize and form individual TJ strands, which adhere to strands of adjacent cells to mediate paracellular sealing (Furuse et al., 1998b, 1999; Kubota et al., 1999). Thereby, the combination and proportion of individual claudins is crucial for the correct formation and tightness of paired TJs, which ultimately control paracellular barrier function (Tsukita and Furuse, 2002).

In *Drosophila* as well as other arthropods, the paracellular epithelial barrier is mediated by a lateral membrane structure, the septate junction (SJ; Tepass et al., 2001). SJs are characterized by a ladder-like arrangement of distinct septa, which interconnect the opposite cell membranes (Tepass et al., 2001; Knust and Bossinger, 2002). Two main types of SJs have been described. Pleated SJs (pSJs), which develop in ectodermally derived tissues, forming regular undulating rows of septa and, in contrast, smooth SJs, which are mainly found in endodermally derived epithelia, forming linear bands of septa (Tepass and Hartenstein, 1994). SJs are also thought to play a role in cell proliferation, cell adhesion, cell communication, and maintenance of cell polarity (Woods et al., 1996; Bilder et al., 2000, 2003; Tepass et al., 2001).

Only a few SJ components of *Drosophila* have been identified. They include the transmembrane protein Neurexin (Nrx), which is specifically required for pSJ formation. The disruption of pSJs in peripheral and subperineural glia cells in *nrx* mutants causes a breakdown of blood-nerve-brain barrier (Baumgartner et al., 1996; Littleton et al., 1997). Nrx interacts with Coracle (Cor) at the cytoplasmic face of SJs (Ward et al., 1998). Cor belongs to the protein 4.1 superfamily of cytoplasmic proteins, which are associated with the plasma membrane (Fehon et al., 1994; Lamb et al., 1998). Like Nrx, Cor is also required for the integrity of transepithelial barrier function (Lamb et al., 1998).

Here we show that a *Drosophila* claudin homolog, Megatrachea (Mega), is localized in pSJs of ectodermally derived epithelia. Its activity is required for transepithelial barrier function and cell shape, but not for cell polarity.

Results

Identification of *megatrachea* Gene

The respiratory organ of *Drosophila*, the tracheal system, exhibits a branched tubular network that is formed of ectodermally derived epithelial tissue. The polarized tracheal cells face the tracheal lumen via their apical membrane, whereas the basolateral domains make contact with the interstitial space of the organism (Affolter and Shilo, 2000; Lubarsky and Krasnow, 2003).

In order to identify genes involved in epithelial formation, we screened an X chromosomal P element collection (Peter et al., 2002) for mutants that affect tracheal branch morphogenesis. Two insertion lines, *P{lacW}l(1)G0012* and *P{lacW}l(1)G0044*, caused elongated and tortuous tracheal branches, most prominent in the main tracheal tube connection, the dorsal trunk (compare Figure 1A with Figure 1B). This mutant phenotype is reminiscent of the tracheal phenotype of *megatrachea* (*mega*) mutant embryos (Beitel and Krasnow, 2000). The P element insertion mutants failed to complement $mega^{EA97}$ and $mega^{VE896}$ (Beitel and Krasnow, 2000),

*Correspondence: rschuh@gwdg.de

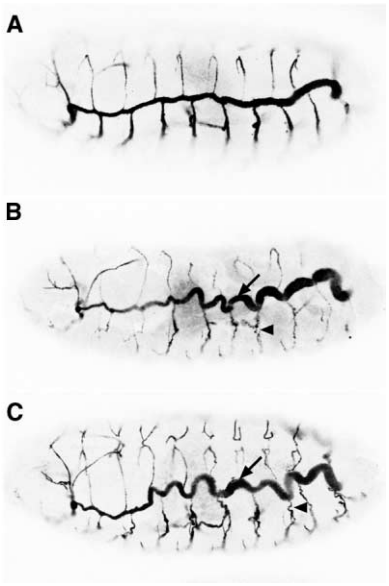

Figure 1. Tracheal Tube Expansion Phenotype of *mega* Alleles

Whole-mount antibody staining of stage 15 wild-type (A), homozygous *P{lacW}l(1)G0012* (B), and transheterozygous *P{lacW}l(1)G0012/Df(1)sta* (C) embryos with antibody 2A12. This antibody specifically stains the tracheal lumen and reveals a tortuous dorsal trunk (arrows in [B] and [C]) and a tortuous transverse connective (arrowheads in [B] and [C]) formation in homozygous *P{lacW}l(1)G0012* (B) and transheterozygous *P{lacW}l(1)G0012/Df(1)sta* (C) embryos. Note: homozygous *P{lacW}l(1)G0044* mutant embryos reveal an equivalent tracheal phenotype as shown in (B) (not shown). Dorsolateral view; anterior is left, dorsal is up.

indicating that the P element insertions have generated new *mega* alleles, referred to as $mega^{G0012}$ and $mega^{G0044}$, respectively. The mutant phenotypes of $mega^{G0012}$ and $mega^{G0044}$ were not enhanced in combination with a *mega* chromosomal deficiency (*Df(1)sta*; Figure 1C; not shown), indicating that $mega^{G0012}$ and $mega^{G0044}$ represent amorphic *mega* alleles.

Both P element insertions reside in a 5′ untranslated region of annotated gene *CG14779*, encoding a putative protein of 256 amino acids (Figures 2A and 2B). The P elements were inserted 23 bp and 83 bp upstream of the putative translation start site, respectively (Figure 2A), and cause lack of both *CG14779* transcript and protein expression (not shown). Mobilization of the P element in $mega^{G0012}$ resulted in several independent excision lines, which reestablished *CG14779* expression and caused reversion of the mutant phenotype. Furthermore, each of the previously identified alleles $mega^{EA97}$ and $mega^{VE896}$ exhibit a single amino acid replacement in the putative *CG14779* protein (for details, see Figure 2C). Collectively, these results indicate that the *CG14779* gene encodes *mega*.

mega Encodes a Claudin-like Protein

Hydrophobicity analysis of the putative Mega protein (see Experimental Procedures) predicts four transmembrane domains that leave both N and C termini located in the cytoplasm (Figure 2C). This structure and sequence similarity predicts Mega as a *Drosophila* member of the claudin family of vertebrate transmembrane proteins (Tsukita and Furuse, 2002; Heiskala et al., 2001). A more detailed sequence comparison of Mega with claudin-10 (Kiuchi-Saishin et al., 2002) and claudin-18 (Niimi et al., 2001) reveals the highest similarity in potential transmembrane domains, the N-terminal extracellular loop and the C-terminal region (Figures 2C and 2D). Interestingly, the C-terminal region of Mega contains a potential PDZ domain-interacting motif (Sheng and Sala, 2001; Figure 2B) also found in most claudins (Itoh et al., 1999). Furthermore, phylogenetic analysis (see Experimental Procedures) reveals that Mega is more homologous to the claudin proteins than to members of the claudin-related BCMP1 and EMP groups of proteins (Christophe-Hobertus et al., 2001).

Thus, Mega encodes a member of the claudin protein family and, thereby, establishes that claudins are conserved in *Drosophila*.

mega Transcript and Protein Expression Pattern during Embryogenesis

To visualize *mega* transcript and Mega protein expression during embryogenesis, we performed in situ hybridization and antibody staining analysis on whole-mount embryos (Experimental Procedures). Transcript and protein are evenly distributed in unfertilized eggs and during cellular blastoderm (not shown; Figure 3A), indicating that Mega is maternally contributed. The generation of germline clones of $mega^{G0012}$ and $mega^{VE896}$ alleles (see Experimental Procedures) revealed that embryos, which lack maternal *mega* function, form a normal tracheal system and develop into fertile adults. Also, embryos that lack both maternal and zygotic *mega* expression develop a tracheal phenotype indistinguishable from that of zygotic mutants (not shown). These results suggest that the maternal aspect of *mega* expression is not essential for normal development or viability. Zygotically expressed *mega* transcript is first observed during stage 11 in the epidermis (not shown; stages according to Campos-Ortega and Hartenstein, 1985) followed by Mega protein expression, which is detectable at stage 12 (Figure 3B). During subsequent embryonic development, the spatial aspects of *mega* transcript and Mega protein expression coincide. They are expressed in ectodermally derived tissues such as epidermis (Figure 3C), tracheal system (Figure 3C), foregut (Figure 3D), hindgut (Figure 3E), and salivary glands (Figure 3E). Mega is not detectable in Malpighian tubules and amnioserosa. By these means, Mega distribution is reminiscent of Nrx and Cor expression (Fehon et al., 1994; Baumgartner et al., 1996). Furthermore, double-labeling experiments reveal coexpression of Mega and Nrx in the scolopales of lateral chordotonal organs (Figures 3F–3H) and in the glia-wrapped axons of the peripheral nervous system (PNS; Figures 3I–3K). The notable difference between Mega and Nrx expression is the segmentally repeated Mega expression, which is only in a subset of Nrx-expressing midline glia cells (Figures 3L–3N). Thus, all tissues that express Mega in the embryo are characterized by the presence of pSJs.

Mega Is Localized in Septate Junctions and Essential for Septae Formation

Coexpression studies of Mega and the cell membrane skeleton marker α-Spectrin (Spec; Dubreuil et al., 1997)

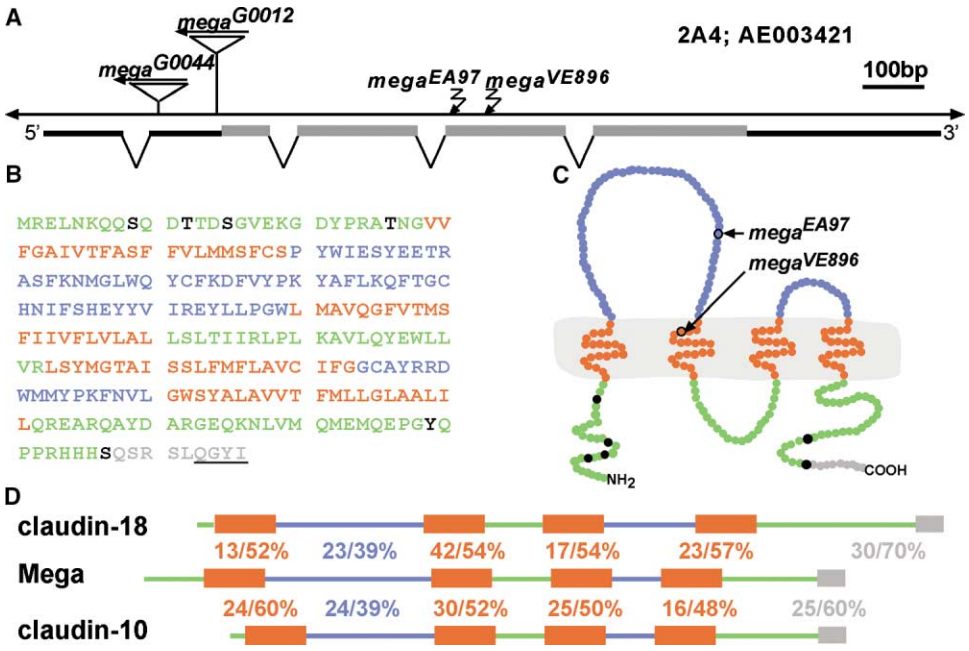

Figure 2. Molecular Organization of *mega* Gene and Putative Mega Protein

(A) Physical map of genomic region 2A4 (GenBank accession number AE003421) containing the *mega* gene. The P elements of the enhancer trap lines $mega^{G0012}$ and $mega^{G0044}$ are inserted in the untranslated region of exon 2. Gray bar: the longest open reading frame (768 bp) of the *mega* transcript. Black bar: untranslated region of the *mega* transcript. The transcribed regions of the EMS-induced $mega^{EA97}$ and $mega^{VE896}$ alleles were sequenced and the detected point mutations are indicated.

(B) Deduced amino acid sequence of putative Mega protein. The predicted transmembrane domains (red), extracellular loops (blue), intracellular loops (green), conserved C-terminal region (gray), and potential PDZ domain-interacting motif (underlined) are indicated. The cytoplasmic region of Mega displays six consensus motifs for phosphorylation by protein kinase C; the potential phosphorylation sites are marked (black).

(C) Diagram showing the predicted membrane (gray) association of Mega. Protein color code is as described in (B). The alleles $mega^{EA97}$ and $mega^{VE896}$ reveal amino acid exchanges (black encircled) in the predicted protein from E to V in position 97 and from V to M in position 113, respectively.

(D) Sequence comparison of Mega (FBgn0025384, Flybase) with claudin-10 (GenBank accession number AF124425) reveals 19% identity and 41% similarity; sequence comparison of Mega with claudin-18 (GenBank accession number AF221068) reveals 20% identity and 37% similarity. Sequence identities and similarities of the various protein domains are indicated. Protein color code is as described in (B).

reveal colocalization in an apicolateral cell membrane region, suggesting a distinct and restricted association of Mega with the membrane (Figure 4A). To further determine the membrane compartment to which Mega is localized, we performed double-labeling experiments with markers for specific membrane compartments. The most apical membrane compartment of epithelial tissues is defined by the marginal zone (Tepass 1996 [also termed subapical region; Knust and Bossinger, 2002; Müller 2003]) stained by anti-Crumbs (Crb) antibodies (Tepass et al., 1990; Tepass 1996). Mega and Crb do not colocalize (Figure 4B). Likewise, a marker for the more basally localized zonula adherens (ZA; Tepass et al., 2001), Armadillo (Arm; Riggleman et al., 1990), reveals no overlap with Mega (Figure 4C). In contrast, SJs (Tepass and Hartenstein, 1994; Tepass et al. 2001), which abut the basal rim of ZA (Knust and Bossinger, 2002) and are characterized by Nrx (Baumgartner et al., 1996) and Cor (Fehon et al., 1994; Ward et al., 1998), reveal precise colocalization of Mega with both Nrx and Cor in all analyzed tissues during embryogenesis (Figures 4D–4I; not shown). Thus, Mega is expressed in pSJs of ectodermally derived epithelia.

To determine whether *mega* is necessary for pSJ formation, we analyzed the cellular localization of the SJ components Nrx, Cor, and FasIII in *mega* mutant embryos. These SJ markers reveal mislocalization along the basolateral cell membrane and are not restricted only to SJs anymore in *mega* mutant embryos (Figures 4J–4L). These observations suggest that the morphology of pSJs is abnormal in the absence of *mega* activity. To test this assumption further, we analyzed the ultrastructural morphology of pSJs in *mega* mutant embryos using transmission electron microscopy (Figures 4M and 4N). Wild-type tracheal cells reveal the typical ladder-like appearance of pSJs (Figure 4M). In contrast, *mega* mutant cells lack the ladder-like septae of pSJs and show instead an intercellular cleft filled with unstructured electron-dense material (Figure 4N; compare with Figure 4M).

These results demonstrate that Mega is an integral component of pSJs and is essential for pSJ morphogenesis.

Mega Is Not Necessary for Epithelial Polarity

We next asked whether Mega participates in epithelial cell polarity. Therefore, we examined the distribution of subcellular membrane markers in epithelial cells of embryos lacking *mega* activity. The polarity markers such as Crb (Tepass et al., 1990), Arm (Riggleman et al.,

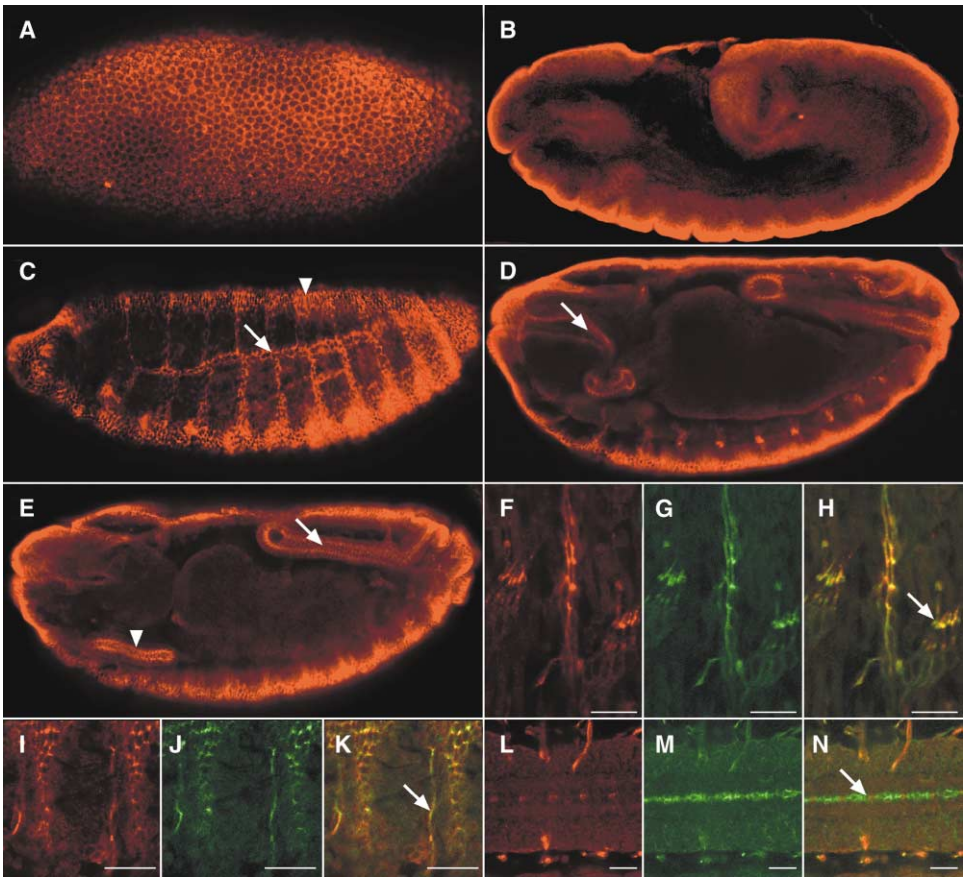

Figure 3. Mega Protein Expression during *Drosophila* Embryonic Development

(A–E) Whole-mount antibody staining of wild-type embryos at stage 5 (A), stage 12 (B), and stage 15 (C–E) using anti-Mega antibodies and visualized by confocal microscopy.

(C–E) Micrographs of the same embryo at different focal planes reveal staining in the tracheal system (arrow in [C]), epidermis (arrowhead in [C]), foregut (arrow in [D]), hindgut (arrow in [E]), and salivary glands (arrowhead in [E]).

(F–N) Whole-mount antibody double staining of stage 15 wild-type embryos using anti-Mega (red) and anti-Nrx (green) antibodies. Single-channel images for Mega (F, I, and L) and Nrx (G, J, and M) expression. Merged images of Mega (red) and Nrx (green) reveal colocalization (yellow; [H, K, and N]) in the scolopales of chordotonal organs (arrow in [H]), in the glia-wrapped axons of the peripheral nervous system (arrow in [K]), and in the segmentally repeated cell clusters of midline glia cells of the central nervous system (arrow in [N]). White bars indicate a size of 10 μm.

1990), Bazooka (Baz; Wodarz et al., 1999), and DmPar-6 (Petronczki and Knoblich, 2001) revealed a normal subcellular localization in *mega* mutant embryos (Figures 5A and 5B, and not shown), indicating that *mega* is involved neither in the establishment nor in the maintenance of epithelial cell polarity.

Mega Is a Functional Component of the Transepithelial Barrier

To examine whether Mega plays a role in the transepithelial barrier, we tested the paracellular flow across epithelial sheets that lack *mega* activity. We analyzed a rhodamine-labeled 10 kDa dextran for its ability to pass the transepithelial barrier of *mega* mutant embryos by injecting the dye into the hemocoel of stage 16 embryos (Lamb et al., 1998; Ward et al., 2001; see Experimental Procedures). In wild-type (n = 65) and heterozygous *mega* mutant embryos (n = 254; $mega^{G0012}$ and $mega^{VE896}$, each balanced over *FM7i, Actin5c-GFP*), the labeled dextran stays confined to the hemocoel and shows no paracellular flow across the epithelial layer of the tracheal system (Figure 5C) and salivary glands (Figure 5G). In homozygous $mega^{G0012}$ (n = 30) and $mega^{VE896}$ (n = 18) mutant embryos, however, the dye rapidly crossed epithelial layers via paracellular flow (Figure 5F) and filled the luminal space of both the tracheal system (Figures 5D and 5E) and salivary glands (Figures 5H and 5I) within 25 min and 45 min, respectively (see Experimental Procedures). These observations demonstrate that Mega functions in either establishment or maintenance of the transepithelial barrier of SJs.

Mega Is Necessary for a Normal Tracheal Cell Shape Formation

The elongated dorsal trunk in *mega* mutant embryos (see above; Beitel and Krasnow, 2000) prompted us to examine dorsal trunk cell shape formation in wild-type and *mega* mutant embryos. Wild-type dorsal trunk cells have a stereotypical cuboidal cell shape (Figure 5J) with a length of 4.7 μm (±1.1 μm; n = 58) and a width of 4.0

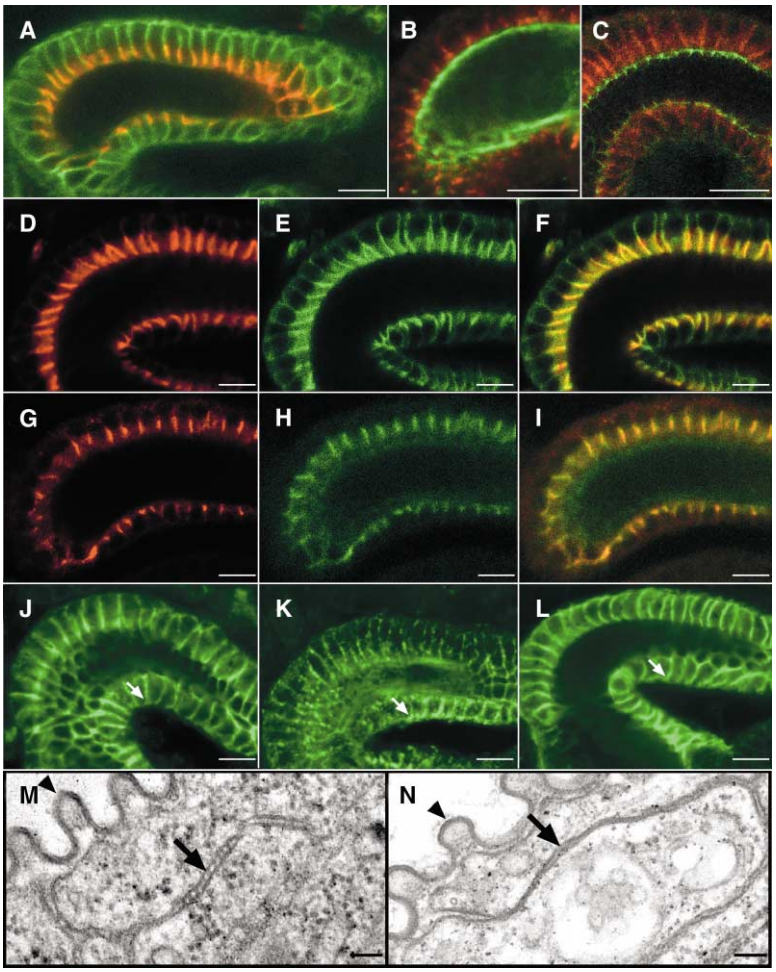

Figure 4. Mega Is Localized to Septate Junctions

(A–C) Whole-mount antibody double staining of stage 15 wild-type embryos using anti-Mega ([A–C]; red) and anti-Spec ([A]; green) or anti-Crb ([B]; green) or anti-Arm ([C]; green) antibodies analyzed in posterior hindgut cells.

(A–C) Mega (red) is restricted to the apicolateral cell membrane as shown by colocalization with the membrane marker Spec ([A]; green). No overlap of Mega ([B and C]; red) localization with Crb ([B]; green), a marker for the apical membrane region, or Arm ([C]; green), a marker for the ZA, is detectable.

(D–I) Whole-mount antibody double staining of stage 15 wild-type embryos using anti-Mega and anti-Cor (D–F) or anti-Nrx (G–I) antibodies. Single-channel images are shown for Mega (D and G) and SJ markers Cor (E) or Nrx (H). Merged images reveal colocalization ([F]; yellow) of Mega (red) and Cor (green) as well as colocalization ([I]; yellow) of Mega (red) and Nrx (green) in posterior hindgut cells. Equivalent colocalization of Mega and Nrx in SJs was observed in all other examined tissues (not shown).

(J–N) Whole-mount antibody staining of stage 15 *mega*^{G0012} mutant embryos using anti-Cor (J), anti-Nrx (K), and anti-FasIII (L) antibodies. Cor (J), Nrx (K), and FasIII (L) are mislocalized along the basolateral cell membrane in *mega* mutant posterior hindgut cells (arrows in [J]–[L]). White bars indicate a size of 10 μm. Transmission electron microscopy of early stage 17 wild-type (M) and *mega*^{G0012} (N) mutant tracheal cells. Septae of pSJs are prominent and regularly spaced in wild-type (arrow in [M]). *mega* mutant embryos lack the septae and instead show unstructured electron-dense material in the intercellular space (arrow in [N]). Taenidial folds of the dorsal trunk are indicated (arrowheads in [M] and [N]). Black bars indicate a size of 100 nm.

μm (±1.0 μm; n = 58), respectively. In contrast, dorsal trunk cells of *mega*^{VE896} mutant embryos display an irregular and stretched shape (Figure 5K) with a length of 6.3 μm (±1.3 μm; n = 48) and a width of 3.3 μm (±0.8 μm; n = 48). Thus, the tracheal cell shape is affected in *mega* mutants, providing an explanation for the tortuous dorsal trunk development in *mega* mutant embryos. However, the cell shape changes are not caused by any prominent defects in cytoskeleton organization, because neither the subcellular localization nor the intensity of GFP-labeled actin and tubulin (Figures 5L–5O), as well as polarization of the microtubule cytoskeleton (Figures 5P and 5Q), is altered in *mega* mutant tracheal cells.

Control of Subcellular Mega Localization by Tube Expansion Genes

mega belongs to the group of tracheal tube expansion genes that affect tube length and diameter size (Beitel and Krasnow, 2000). We therefore examined Mega tissue distribution and its subcellular localization in embryos that are mutant for tube expansion genes. Mega is distributed normally in embryos that are homozygous mutant for *bulbous* (*bulb*), *convoluted* (*conv*), *cystic* (*cyst*), and *varicose* (*vari*; not shown). In contrast, in *sinuous* (*sinu*) mutant embryos, Mega is mislocalized to a basolateral position at the tracheal cell membrane (compare Figure 6A with Figure 6B). Interestingly, Mega is also mislocalized in the hindgut (compare Figure 4D with Figure 6C), salivary glands, and epidermis (not shown) of such embryos, suggesting that *sinu* might be involved in the development of these ectodermal tissues as well. The observations suggest that *sinu* activity participates in targeting Mega to SJs, whereas the other tube expansion genes may act in a manner independent of Mega to mediate normal tracheal tube formation.

Neurexin and Coracle Are Involved in Subcellular Localization of Mega

The specific localization of Mega in SJs suggests its interaction with SJ-associated proteins. To test this proposal, we examined the subcellular localization of Mega in embryos that lack the septate junction components Cor, FasciclinIII (FasIII; Woods et al., 1997), and Nrx. Although still membrane associated, Mega shows a basolateral distribution rather than being tightly associated

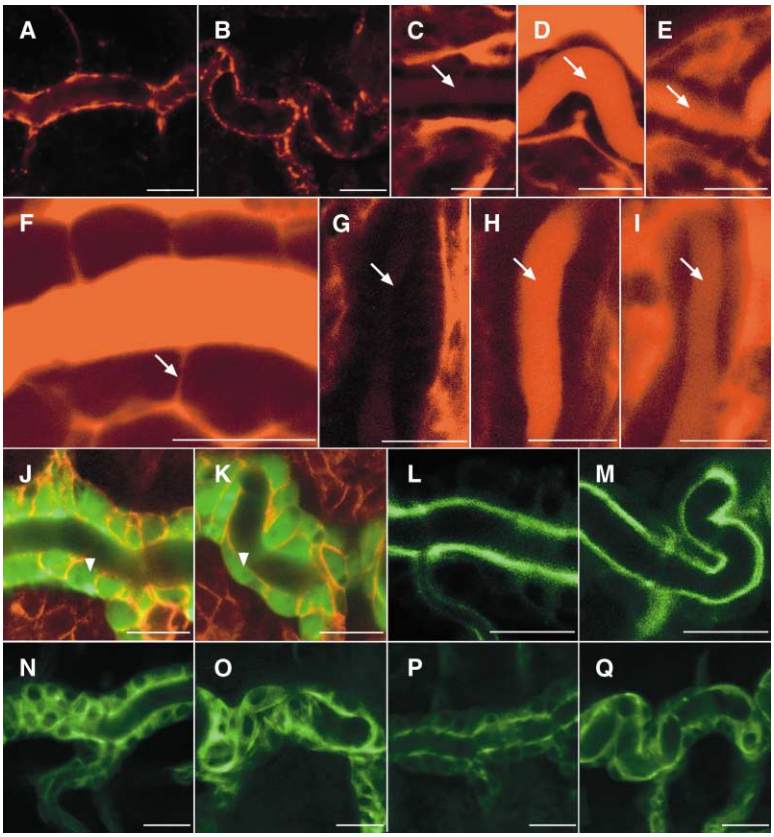

Figure 5. The Transepithelial Barrier Function and Tracheal Cell Shape Formation Are Affected in *mega* Mutant Embryos

(A–I) Whole-mount antibody staining of stage 15 wild-type (A) and $mega^{G0012}$ (B) embryos using anti-Crb antibodies. Crb is apically localized in *mega* mutant tracheal cells (B) as in wild-type tracheal cells (A). Confocal images of tracheal dorsal trunk branches (C–F) or salivary glands (G–I) of $mega^{VE896}$/FM7 (C), $mega^{G0012}$ (D, F, and H), $mega^{VE896}$ (E and I), and wild-type (G) stage 16 embryos after rhodamine-dextran injection into the hemocoel (see Experimental Procedures). Wild-type and heterozygous $mega^{VE896}$/FM7 embryos reveal no diffusion of rhodamine-dextran into the tubular structures of the tracheal system (arrow in [C]) and salivary glands (arrow in [G]) 90 min after injection. In contrast, homozygous $mega^{G0012}$ and $mega^{VE896}$ embryos show diffusion into the lumen of the tracheal system (arrows in [D] and [E]; images 25 min after injection) and salivary glands (arrows in [H] and [I]; images 45 min after injection). Homozygous $mega^{G0012}$ embryos reveal transepithelial rhodamine-dextran diffusion into the tracheal lumen 20 min after injection (arrow in [F]).

(J and K) Whole-mount antibody double staining of stage 16 *1-eve-1* (J) and *1-eve-1;* $mega^{VE896}$ (K) embryos using anti-β-galactosidase (green) and anti-Spec (red) antibodies. The β-galactosidase expression of the *1-eve-1* line marks the tracheal cells, and Spec expression in cell membranes reveals the cell shape. Normal tracheal dorsal trunk cells are cubically shaped (arrowhead in [J]), while homozygous $mega^{VE896}$ tracheal cells show elongated cell shapes (arrowhead in [K]).

(L–Q) Whole-mount GFP in vivo visualization of stage 16 wild-type (L and N) and $mega^{G0044}$ (M and O) mutant embryos bearing *btl-GAL4* and *UAS-actin-GFP* (L and M) or *UAS-tau-myc-GFP* (N and O). Whole-mount anti-β-galactosidase antibody staining of stage 16 wild-type (P) and $mega^{G0044}$ (Q) mutant embryos bearing *btl-GAL4* and *UAS-Nod-lacZ*. The Nod:β-gal fusion protein is a minus end reporter for microtubules localized to apical cytoplasm in epithelial cells (Clark et al., 1997). No prominent changes are detectable in intracellular actin (M), in tubulin cytoskeleton (O), and in polarization of microtubules (Q) in tracheal cells of *mega* mutant embryos. White bars indicate a size of 10 μm.

with SJs in *cor* as well as in *nrx* mutant embryos (Figures 6D and 6E). In contrast, Mega appears to be normally localized in *fasIII* mutant embryos (Figure 6F). This difference suggests that the proper targeting of Mega to the SJs depends on both *cor* and *nrx* and is independent of *fasIII* activity.

Previous observations revealed that Cor and Nrx directly interact with and depend on each other for an SJ localization (Ward et al., 1998). Thus, the results imply that Mega requires an interaction with Cor/Nrx or a Cor/Nrx-dependent component for its targeting. This conclusion is supported by overexpression experiments (Figures 6G–6O) showing that *UAS/GAL4*-driven (Brand and Perrimon, 1993) *mega* activity in the hindgut (*UAS-mega*; *G455-GAL4*) causes Mega accumulation predominantly along the lateral membrane regions (Figures 6G, 6J, and 6M). This ectopic Mega localization coincides precisely with Cor (Figures 6H and 6I) and Nrx (Figures 6K and 6L) membrane localization, indicating that mislocalization of Mega causes also mislocalization of the Cor/Nrx complex. In contrast, Mega overexpression does not cause an ectopic localization of FasIII (Figures 6N and 6O). Thus, the results suggest an either direct or indirect interaction of Mega with the Cor/Nrx complex.

Discussion

We present evidence that the *Drosophila* gene *mega* encodes a transmembrane protein that is structurally and functionally similar to the family of claudin proteins in vertebrates.

The Role of *mega* in Septate Junctions

Mega is localized to SJs of primary epithelia about 1 hr before they become morphologically distinct (Tepass and Hartenstein, 1994). SJs execute various functions, which include cell-cell adhesion and cell morphology. Also, the SJ components Scribble and Discs large are necessary to control basolateral membrane organization (Bilder et al., 2003). Most importantly, SJs provide a transepithelial barrier and direct paracellular flow of materials across epithelia (Tepass et al., 2001). Our results indicate that Mega participates in the distinctive functional properties of SJs.

Embryos that lack *mega* function reveal a normal distribution of apicobasal cell polarity markers. Mega is, therefore, not involved in organization or maintenance of epithelial polarity. In addition, integrity of epidermal sheets is not affected by *mega*, because *mega* mutants

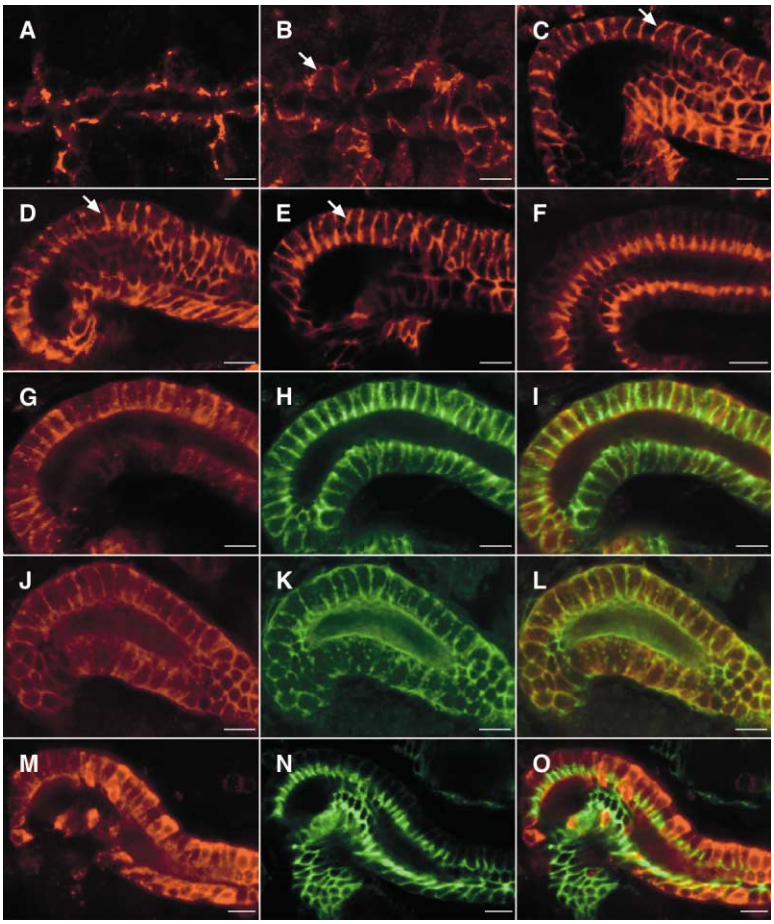

Figure 6. Subcellular Mega Localization Depends on *sinu*, *cor*, and *nrx*

(A–F) Whole-mount antibody staining of stage 16 wild-type (A), *sinu*^{06524} (B and C), *cor*^{5} (D), *nrx*^{4304} (E), and *fasIII*^{E25} (F) mutant embryos using anti-Mega antibodies and visualized by confocal microscopy. *sinu*, *cor*, and *nrx* mutant embryos reveal mislocalization of Mega (arrows in [B]–[E]) along the basolateral cell membrane of trachea ([B], and not shown) and posterior midgut cells (C–E). *fasIII* mutant embryos show a normal Mega localization in posterior hindgut cells (F).

(G–L) Whole-mount antibody double staining of stage 15 embryos bearing *UAS-mega* and *G455-GAL4* with anti-Mega (G–O) and anti-Cor (G–I) or anti-Nrx (J–L) or anti-FasIII (M–O) antibodies visualized by confocal microscopy. Merged images of Mega (red; [G]) and Cor (green; [H]) expression as well as Mega (red; [J]) and Nrx (green; [K]) expression reveal ectopic coexpression of Mega and Cor (yellow; [I]) as well as Mega and Nrx (yellow; [L]). In contrast, FasIII shows a wild-type-like localization (green; [N and O]) in the presence of ectopic Mega expression (red; [M and O]). The white bar indicates a size of 10 μm.

develop coherent ectodermal organs and tissues. In contrast, *mega* is necessary for normal tracheal cell formation. The stereotyped cuboidal cell shape of dorsal trunk cells is lost in *mega* mutant embryos and cells exhibit an irregular stretched morphology instead. How is cell shape formation controlled by Mega? Our results indicate that the tubulin distribution and the apical concentration of actin bundles (Lee and Kolodziej, 2002) are not affected in *mega* mutant epithelial cells, suggesting that there are no prominent changes in the actin and tubulin cytoskeleton. On the other hand, the localization of Mega to SJs depends on Nrx and Cor, which might provide a link between SJ components and cytoskeleton structures, because the vertebrate homolog of Cor, the membrane-skeleton protein 4.1, crosslinks plasma membrane to the underlying cytoskeleton through protein-protein interactions (Hoover and Bryant, 2000). Also, the PDZ binding motif found in the C terminus of Mega represents a bona fide protein interaction motif for binding a PDZ repeat-containing protein, such as members of MAGUK class, which assemble specific protein complexes by linking membrane and cytoplasmic proteins (Sheng and Sala, 2001). Thus, it might be possible that lack of *mega* activity may affect the connectivity of SJs with cytoskeleton structures that consequently results in the irregular shaped cells.

The most intriguing function of SJs is their role in the formation of a transepithelial diffusion barrier (Tepass et al., 2001). Our fluorescent dye diffusion experiments demonstrate that Mega is required for the barrier function of SJs, and thus affects the same SJ property as described for Cor and Nrx (Baumgartner et al., 1996; Lamb et al., 1998; Ward et al., 2001). This feature together with the expression pattern similarities and the Cor/Nrx-dependent localization of Mega outlines a close functional relationship between the three proteins, leaving open the question of whether they tune the tightness and/or selectivity of SJs. Time course diffusion experiments in mutant embryos combined with differently sized dyes may elucidate a possible specificity of the SJ components and answer the question of whether they selectively regulate paracellular flow.

Tracheal Tube Size Control

Tracheal tube size formation is a tightly controlled process that underlies a defined genetic program (Beitel and Krasnow, 2000). Recently, it has been shown that the transcription factor Grainy head (Grh) controls apical membrane enlargement of tracheal cells. Lack of *grh* activity causes apical membrane overgrowth that leads to tube elongation. Also, mutations of the cell adhesion protein FasciclinII (FasII) and the sodium/potassium-transporting ATPase α subunit (ATPα) affect the lateral cell surface, which results in cell shape changes and

consequently, in extended tubes (Hemphälä et al., 2003). We identified the SJ component Mega to be essential for tube elongation as well. The disruption of SJs in *mega* mutant embryos may expand the apical cell surface at the expense of the lateral surface. Thus, specific subcellular compartments seem to be critical for the establishment of tracheal tube length and size.

Claudins Are Essential Components of Septate Junctions and Tight Junctions

Claudins are the major transmembrane molecules of TJ complexes in epithelial cells of vertebrates (Furuse et al., 1998b; Gow et al., 1999; Morita et al., 1999). While invertebrates lack TJs, it has been discussed that SJs display equivalent functions (Baumgartner et al., 1996; Tepass et al., 2001). We provide evidence that Mega represents a *Drosophila* claudin-like protein. Mega is specifically localized in SJs and, thus, SJs and TJs contain similar structural components. Moreover, Mega and claudins share functional similarities, as both participate in the barrier function as demonstrated by the red dextran injection experiments in *mega* mutants and by the tracer experiments in claudin-1-deficient mice (Furuse et al., 2002). These findings suggest an analogous function of Mega in SJs as observed for the claudins in TJs.

Do Claudin-like Proteins Comprise a Protein Family in *Drosophila*?

The claudin family consists of 24 members in mammals and 15 in zebrafish (Kollmar et al., 2001; Tsukita and Furuse, 2002). Outside the phylum Chordata, sequences with significant similarity to claudins have been identified recently in *Caenorhabditis elegans* (Asano et al., 2003; Simske et al., 2003). Our demonstrations of the structural and functional features of Mega imply that claudin function is conserved in *Drosophila*. Moreover, homology searches with *mega* sequences revealed four additional putative claudin-like genes in *Drosophila* (unpublished results). Based on genomic localization data, one of these genes might be *sinu*, which belongs to the same tracheal tube expansion gene family as *mega* (Beitel and Krasnow, 2000) and participates in the subcellular localization of Mega. It will be interesting to see whether *sinu* and the additional claudin-like genes encode transmembrane proteins that are localized in SJs and function in a way similar to Mega. These analyses include questions concerning the role of each of the claudin-like genes and whether or not they can partially replace each other's functions. Answers to these questions are also relevant for the vertebrate system, where combinations of distinct claudin family members have been proposed to specify the tightness of the junctional complex (Tsukita and Furuse, 2002). Due to the small number of claudin-like proteins and the genetic tools available, *Drosophila* provides an ideal system in which the function of claudins and the possible functional combinations among them can be addressed.

Experimental Procedures

Antibodies, Immunofluorescence, and In Situ Hybridization

Anti-Mega antibodies against the peptides MRELNKQQSQDTTDS (amino acids 1–15) and GYQPPRHHHSQSRSL (amino acids 238–252) were generated in rabbit and guinea pig at Eurogentec. Rabbit anti-Mega antibody was used at 1:25 dilution and guinea pig anti-Mega antibody at 1:30 dilution. Additional antibodies were used, as follows: 2A12 (1:5) to stain the tracheal lumen, anti-Arm (1:5; Riggleman et al., 1990), anti-Crb (1:10; Tepass et al., 1990), anti-FasIII (1:10; Patel et al., 1987), and anti-α-Spec (1:5; Dubreuil et al., 1997) were obtained from the Developmental Studies Hybridoma Bank (DSHB). We also used rabbit anti-Baz (1:500; Wodarz et al., 1999; gift from E. Knust), guinea pig anti-Cor (1:2000; Fehon et al., 1994; gift from R.G. Fehon), rabbit anti-Nrx (1:500; Baumgartner et al., 1996; gift from H.J. Bellen), and rabbit anti-DmPar-6 (1:500; Petronczki and Knoblich, 2001; gift from J.A. Knoblich). Secondary antibodies were obtained from Cappel, Molecular Probes, and Vector Laboratories. For signal amplification, the horseradish peroxidase Elite ABC kit (Vector Laboratories) and the TSA Cyanine 3 system (NEN) were used. Fluorescent immunostainings and RNA in situ hybridizations were performed and analyzed as described (Wolf and Schuh, 2000).

Dextran Red Permeability Experiments

Dechorionated homozygous *mega* mutant embryos at stage 16 were identified by the *FM7i, P{Actin5c-GFP}* balancer chromosome and covered with voltalev oil for injection. Rhodamine-labeled dextran (MW 10,000; Molecular Probes) was purified and injected into the hemocoel of embryos as described by Lamb et al. (1998). The embryos were analyzed by confocal microscopy. First indications of dextran filling in the tracheal lumen were observed after 3 min and in the salivary gland lumen after 10 min. Maximum dye filling was visible after 25 min in the trachea and after 45 min in the salivary glands. Wild-type embryos lack detectable dye filling in the trachea and the salivary glands within 90 min.

Electron Microscopy

After devitellinization, the embryos were fixed by immersion using 2.5% glutaraldehyde in 0.1 M cacodylate buffer (pH 7.4). Fixation of the embryos was performed for 10 min at room temperature before they were bisected midway between anterior and posterior and fixed overnight in 2% glutaraldehyde at 4°C. After postfixation in 1% osmium tetroxide and preembedding staining with 1% uranyl acetate, tissue samples were dehydrated and embedded in Agar100. Thin sections (30–60 nm) were counterstained with uranyl acetate and lead citrate and examined using a Philips CM 120 BioTwin transmission electron microscope (Philips Inc.). Images were taken with a 1 K slow scan CCD camera (GATAN, Inc.).

Size and Structure Analysis

Fluorescent stained embryos were examined by z-scan analysis as described (Wolf et al., 2002) and dorsal trunk and cell size were measured with Archi Cad 6.5 (GRAPHISOFT). Statistic calculations were performed with Microsoft Excel 98.

Mega protein structure was examined by the programs TMHMM2.0 (transmembrane hidden Markov model), DAS (dense alignment surface); NetPhos, and Signal-IP, and the servers CBS (Center for Biological Sequence Analysis; http://www.cbs.dtu.dk/services), the PredictProtein server (http://cubic.bioc.columbia.edu/pp/), and SMART (Simple Modular Architecture Research Tool; http://smart.embl-heidelberg.de). Phylogenetic analyses were performed with MegAlign (DNASTAR).

Flystocks

The fly strains *mega*^{VE896}, *bulb*^{k11012b}, *fasIII*^{E25}, *Nrx*^{4304}, *sinu*^{06524}, *vari*^{03953b}, *69B-GAL4*, and *Actin5c-GAL4* were obtained from the Bloomington Stock Center. We also used the strains *mega*^{EA97} (gift from G.J. Beitel); *cor*^{5} (gift from R.G. Fehon); *G455-GAL4* (gift from M. Hoch); *mega*^{G0012}and *mega*^{G0044} (gift from U. Schäfer); *cyst*^{k13717b} and *conv*^{k06507b} (gift from T. Laverty); *UAS-Nod-lacZ* (gift from I.E., Clark); and *btl-GAL4*; *UAS-actin-GFP* and *UAS-tau-myc-GFP*.

To generate germline clones, *mega*^{VE896} and *mega*^{G0012} were recombined onto *P{FRT}101* and recombinants were crossed to *ovo*^{D1}*P{FRT}101/Y;P{hsFLP)38* males. Mitotic recombination was induced by single heat shocks (60 min, 37°C) during early first and second instar larval development. Females with mitotic recombination were identified by eye shape and color and were crossed to

OreR or *FM7c, P{ftz-lacZ}* for mutant analysis or to *FM7i, P{Actin5c-GFP}* for analysis of viability.

Acknowledgments

We thank G.J. Beitel, H.J. Bellen, P.J. Bryant, I.E. Clark, R.G. Fehon, M. Hoch, J.A. Knoblich, E. Knust, T. Laverty, U. Schäfer, and the Bloomington *Drosophila* Stock Center for scientific material. We are grateful to G.J. Beitel, M. Hoch, H. Jäckle, C. Krause, and the members of department Molekulare Entwicklungsbiologie for comments on the manuscript and for discussions. This work was supported by the Max-Planck-Society (MPIbpc Abt.170) and Deutsche Forschungsgemeinschaft (Graduiertenkolleg "Molekulare Genetik der Entwicklung").

Received: April 7, 2003
Revised: July 21, 2003
Accepted: July 23, 2003
Published: October 6, 2003

References

Affolter, M., and Shilo, B.Z. (2000). Genetic control of branching morphogenesis during *Drosophila* tracheal development. Curr. Opin. Cell Biol. *12*, 731–735.

Asano, A., Asano, K., Sasaki, H., Furuse, M., and Tsukita, S. (2003). Claudins in *Caenorhabditis elegans*: their distribution and barrier function in the epithelium. Curr. Biol. *13*, 1042–1046.

Baumgartner, S., Littleton, J.T., Broadie, K., Bhat, M.A., Harbecke, R., Lengyel, J.A., Chiquet-Ehrismann, R., Prokop, A., and Bellen, H.J. (1996). A *Drosophila neurexin* is required for septate junction and blood-nerve barrier formation and function. Cell *87*, 1059–1068.

Beitel, G.J., and Krasnow, M.A. (2000). Genetic control of epithelial tube size in the *Drosophila* tracheal system. Development *127*, 3271–3282.

Bilder, D., Li, M., and Perrimon, N. (2000). Cooperative regulation of cell polarity and growth by *Drosophila* tumor suppressors. Science *289*, 113–116.

Bilder, D., Schober, M., and Perrimon, N. (2003). Integrated activity of PDZ protein complexes regulates epithelial polarity. Nat. Cell Biol. *5*, 53–58.

Brand, A.H., and Perrimon, N. (1993). Targeted gene expression as a means of altering cell fates and generating dominant phenotypes. Development *118*, 401–415.

Campos-Ortega, J.A., and Hartenstein, V. (1985). The Embryonic Development of *Drosophila melanogaster* (Berlin: Springer).

Christophe-Hobertus, C., Szpirer, C., Guyon, R., and Christophe, D. (2001). Identification of the gene encoding brain cell membrane protein I (BCMPI), a putative four-transmembrane protein distantly related to the peripheral myelin protein 22/epithelial membrane proteins and the claudins. BMC Genomics *2*, 3.

Clark, I.E., Jan, L.Y., and Jan, Y.N. (1997). Reciprocal localization of Nod and kinesin fusion proteins indicates microtubule polarity in the *Drosophila* oocyte, epithelium, neuron and muscle. Development *124*, 461–470.

Dubreuil, R.R., Maddux, P.B., Grushko, T.A., and MacVicar, G.R. (1997). Segregation of two spectrin isoforms: polarized membrane-binding sites direct polarized membrane skeleton assembly. Mol. Biol. Cell *8*, 1933–1942.

Fehon, R.G., Dawson, I.A., and Artavanis-Tsakonas, S. (1994). A *Drosophila* homologue of membrane-skeleton protein 4.1 is associated with septate junctions and is encoded by the *coracle* gene. Development *120*, 545–557.

Furuse, M., Fujita, K., Hiiragi, T., Fujimoto, K., and Tsukita, S. (1998a). Claudin-1 and -2: novel integral membrane proteins localizing at tight junctions with no sequence similarity to occludin. J. Cell Biol. *141*, 1539–1550.

Furuse, M., Sasaki, H., Fujimoto, K., and Tsukita, S. (1998b). A single gene product, claudin-1 or -2, reconstitutes tight junction strands and recruits occludin in fibroblasts. J. Cell Biol. *143*, 391–401.

Furuse, M., Sasaki, H., and Tsukita, S. (1999). Manner of interaction of heterogeneous claudin species within and between tight junction strands. J. Cell Biol. *147*, 891–903.

Furuse, M., Hata, M., Furuse, K., Yoshida, Y., Haratake, A., Sugitani, Y., Noda, T., Kubo, A., and Tsukita, S. (2002). Claudin-based tight junctions are crucial for the mammalian epidermal barrier: a lesson from *claudin-1*-deficient mice. J. Cell Biol. *156*, 1099–1111.

Gow, A., Southwood, C.M., Li, J.S., Pariali, M., Riordan, G.P., Brodie, S.E., Danias, J., Bronstein, J.M., Karchar, B., and Lazzarini, R.A. (1999). CNS myelin and Sertoli cell tight junction strands are absent in *Osp/Claudin-11* null mice. Cell *99*, 649–659.

Heiskala, M., Peterson, P.A., and Yang, Y. (2001). The roles of claudin superfamily proteins in paracellular transport. Traffic *2*, 93–98.

Hemphälä, J., Uv, A., Cantera, R., Bray, S., and Samakovlis, C. (2003). Grainy head controls apical membrane growth and tube elongation in response to Branchless/FGF signalling. Development *130*, 249–258.

Hoover, K.B., and Bryant, P.J. (2000). The genetics of the protein 4.1 family: organizers of the membrane and cytoskeleton. Curr. Opin. Cell Biol. *12*, 229–234.

Itoh, M., Furuse, M., Morita, K., Kubota, K., Saitou, M., and Tsukita, S. (1999). Direct binding of three tight junction-associated MAGUKs, ZO-1, ZO-2, and ZO-3, with the COOH termini of claudins. J. Cell Biol. *147*, 1351–1363.

Kiuchi-Saishin, Y., Gotoh, S., Furuse, M., Takasuga, A., Tano, Y., and Tsukita, S. (2002). Differential expression patterns of claudins, tight junction membrane proteins, in mouse nephron segments. J. Am. Soc. Nephrol. *13*, 875–886.

Knust, E., and Bossinger, O. (2002). Composition and formation of intercellular junctions in epithelial cells. Science *298*, 1955–1959.

Kollmar, R., Nakamura, S.K., Kappler, J.A., and Hudspeth, A.J. (2001). Expression and phylogeny of claudins in vertebrate primordia. Proc. Natl. Acad. Sci. USA *98*, 10196–10201.

Kubota, K., Furuse, M., Sasaki, H., Sonoda, N., Fujita, K., Nagafuchi, A., and Tsukita, S. (1999). Ca^{2+}-independent cell-adhesion activity of claudins, a family of integral membrane proteins localized at tight junctions. Curr. Biol. *9*, 1035–1038.

Lamb, R.S., Ward, R.E., Schweizer, L., and Fehon, R.G. (1998). *Drosophila* coracle, a member of the protein 4.1 superfamily, has essential structural functions in the septate junctions and developmental functions in embryonic and adult epithelial cells. Mol. Biol. Cell *9*, 3505–3519.

Lee, S., and Kolodziej, P.A. (2002). The plakin Short Stop and the RhoA GTPase are required for E-cadherin-dependent apical surface remodeling during tracheal tube fusion. Development *129*, 1509–1520.

Littleton, J.T., Bhat, M.A., and Bellen, H.J. (1997). Deciphering the function of *neurexins* at cellular junctions. J. Cell Biol. *137*, 793–796.

Lubarsky, B., and Krasnow, M.A. (2003). Tube morphogenesis: making and shaping biological tubes. Cell *112*, 19–28.

Morita, K., Furuse, M., Fujimoto, K., and Tsukita, S. (1999). Claudin multigene family encoding four-transmembrane domain protein components of tight junction strands. Proc. Natl. Acad. Sci. USA *96*, 511–516.

Müller, H.A. (2003). Epithelia polarity in flies: more than just Crumbs. Dev. Cell *4*, 1–9.

Niimi, T., Nagashima, K., Ward, J.M., Minoo, P., Zimonjic, D.B., Popescu, N.C., and Kimura, S. (2001). claudin-18, a novel downstream target gene for the T/EBP/NKX2.1 homeodomain transcription factor, encodes lung- and stomach-specific isoforms through alternative splicing. Mol. Cell. Biol. *21*, 7380–7390.

Patel, N.H., Snow, P.M., and Goodman, C.S. (1987). Characterization and cloning of Fasciclin III: a glycoprotein expressed on a subset of neurons and axon pathways in *Drosophila*. Cell *48*, 975–988.

Peter, A., Schottler, P., Werner, M., Beinert, N., Dowe, G., Burkert, P., Mourkioti, F., Dentzer, L., He, Y., Deak, P., et al. (2002). Mapping and identification of essential gene functions on the X chromosome of *Drosophila*. EMBO Rep. *3*, 34–38.

Petronczki, M., and Knoblich, J.A. (2001). DmPAR-6 directs epithelial

polarity and asymmetric cell division of neuroblasts in *Drosophila*. Nat. Cell Biol. *3*, 43–49.

Riggleman, B., Schedl, P., and Wieschaus, E. (1990). Spatial expression of the *Drosophila* segment polarity gene armadillo is posttranscriptionally regulated by wingless. Cell *63*, 549–560.

Rodriguez-Boulan, E., and Nelson, W.J. (1989). Morphogenesis of the polarized epithelial cell phenotype. Science *245*, 719–725.

Schneeberger, E.E., and Lynch, R.D. (1992). Structure, function, and regulation of cellular tight junctions. Am. J. Physiol. *262*, L647–L661.

Sheng, M., and Sala, C. (2001). PDZ domains and the organization of supramolecular complexes. Annu. Rev. Neurosci. *24*, 1–29.

Simon, D.B., Lu, Y., Choate, K.A., Velazquez, H., Al-Sabban, E., Praga, M., Casari, G., Bettinelli, A., Colussi, G., Rodriguez-Soriano, J., et al. (1999). Paracellin-1, a renal tight junction protein required for paracellular Mg^{2+} resorption. Science *285*, 103–106.

Simske, J.S., Köppen, M., Sims, P., Hodgkin, J., Yonkof, A., and Hardin, J. (2003). The cell junction protein VAB-9 regulates adhesion and epidermal morphology in *C. elegans*. Nat. Cell Biol. *5*, 619–625.

Sonoda, N., Furuse, M., Sasaki, H., Yonemura, S., Katahira, J., Horiguchi, Y., and Tsukita, S. (1999). *Clostridium perfingens* enterotoxin fragment removes specific claudins from tight junction strands: evidence for direct involvement of claudins in tight junction barrier. J. Cell Biol. *147*, 195–204.

Tepass, U. (1996). Crumbs, a component of the apical membrane, is required for zonula adherens formation in primary epithelia of *Drosophila*. Dev. Biol. *177*, 217–225.

Tepass, U., and Hartenstein, V. (1994). The development of cellular junctions in the *Drosophila* embryo. Dev. Biol. *161*, 563–596.

Tepass, U., Theres, C., and Knust, E. (1990). crumbs encodes an EGF-like protein expressed on apical membranes of *Drosophila* epithelial cells and required for organization of epithelia. Cell *61*, 787–799.

Tepass, U., Tanentzapf, G., Ward, R., and Fehon, R. (2001). Epithelial cell polarity and cell junctions in *Drosophila*. Annu. Rev. Genet. *35*, 747–784.

Tsukita, S., and Furuse, M. (2002). Claudin-based barrier in simple and stratified cellular sheets. Curr. Opin. Cell Biol. *14*, 531–536.

Tsukita, S., Furuse, M., and Itoh, M. (2001). Multifunctional strands in tight junctions. Nat. Rev. Mol. Cell Biol. *2*, 285–293.

Ward, R.E., Lamb, R.S., and Fehon, R.G. (1998). A conserved functional domain of *Drosophila coracle* is required for localization at the septate junction and has membrane-organizing activity. J. Cell Biol. *140*, 1463–1473.

Ward, R.E., Schweizer, L., Lamb, R.S., and Fehon, R.G. (2001). The protein 4.1, ezrin, radixin, moesin (FERM) domain of *Drosophila* Coracle, a cytoplasmic component of the septate junction, provides functions essential for embryonic development and imaginal cell proliferation. Genetics *159*, 219–228.

Wodarz, A., Ramrath, A., Kuchinke, U., and Knust, E. (1999). Bazooka provides an apical cue for Inscuteable localization in *Drosophila* neuroblasts. Nature *402*, 544–547.

Wolf, C., and Schuh, R. (2000). Single mesodermal cells guide outgrowth of ectodermal tubular structures in *Drosophila*. Genes Dev. *14*, 2140–2145.

Wolf, C., Gerlach, N., and Schuh, R. (2002). *Drosophila* tracheal system formation involves FGF-dependent cell extensions contacting bridge-cells. EMBO Rep. *3*, 563–568.

Woods, D.F., Hough, C., Peel, D., Callaini, G., and Bryant, P.J. (1996). Dlg protein is required for junction structure, cell polarity, and proliferation control in *Drosophila* epithelia. J. Cell Biol. *134*, 1469–1482.

Woods, D.F., Wu, J.-W., and Bryant, P.J. (1997). Localization of proteins to the apico-lateral junctions of *Drosophila* epithelia. Dev. Genet. *20*, 111–118.